

The Surface Detector System of the Pierre Auger Observatory

I. Allekotte^a, A. F. Barbosa^d, P. Bauleo^ℓ, C. Bonifazi^d,
B. Civit^c, C. O. Escobar^e, B. García^c, G. Guedes^f,
M. Gómez Berisso^a, J. L. Harton^ℓ, M. Healy^k, M. Kaducak^j,
P. Mantsch^j, P. O. Mazur^j, C. Newman-Holmes^j, I. Pepe^g,
I. Rodríguez-Caboⁱ, H. Salazar^h, N. Smetniansky-De Grande^b,
D. Warner^ℓ, for the Pierre Auger Collaboration^m

^a*Instituto Balseiro and Centro Atómico Bariloche (U.N. Cuyo and CNEA, CONICET), 8400 Bariloche, Argentina*

^b*Laboratorio Tandem, Comisión Nacional de Energía Atómica and CONICET, Av. Gral. Paz 1499 (1650) San Martín, Buenos Aires, Argentina*

^c*Universidad Tecnológica Nacional Regional Mendoza, Mendoza, Argentina*

^d*CBPF, Rua Xavier Sigaud 150, Rio de Janeiro, Brazil*

^e*Universidade Estadual de Campinas, Instituto de Física, Departamento de Raios Cósmicos, CP 6165, 13084-971, Campinas SP, Brazil*

^f*Universidade Estadual de Feira de Santana (UEFS), Av. Universitaria Km 03 da BR 116, Campus Universitário, 44031-460 Feira de Santana BA, Brazil*

^g*Universidade Federal da Bahia, Campus de Odina, 40210-340 Salvador BA, Brazil*

^h*Benemérita Universidad Autónoma de Puebla (BUAP), Ap. Postal J-48, 72500 Puebla, Puebla, Mexico*

ⁱ*Dpto. Física de Partículas, Universidad de Santiago de Compostela, 15706 Santiago de Compostela, Spain*

^j*Fermi National Accelerator Lab., Batavia IL, U.S.A.*

^k*University of California, Los Angeles (UCLA), Department of Physics and Astronomy, Los Angeles, CA 90095, U.S.A.*

^ℓ*Colorado State University, Fort Collins, CO 80523, U.S.A.*

^m*Pierre Auger Collaboration, Av. San Martín Norte 306, 5613 Malargüe, Mendoza, Argentina*

Abstract

The Pierre Auger Observatory is designed to study cosmic rays with energies greater than 10^{19} eV. Two sites are envisaged for the observatory, one in each hemisphere,

for complete sky coverage. The southern site of the Auger Observatory, now approaching completion in Mendoza, Argentina, features an array of 1600 water-Cherenkov surface detector stations covering 3000 km², together with 24 fluorescence telescopes to record the air shower cascades produced by these particles. The two complementary detector techniques together with the large collecting area form a powerful instrument for these studies. Although construction is not yet complete, the Auger Observatory has been taking data stably since January 2004 and the first physics results are being published. In this paper we describe the design features and technical characteristics of the surface detector stations of the Pierre Auger Observatory.

Key words: Pierre Auger Observatory; high-energy cosmic rays; surface detector array; water-Cherenkov detectors

1 Introduction

Cosmic rays with energies near 10²⁰ eV have been a continuing mystery since Linsley reported the first such event in 1963 [1]. As yet there are no identified sources and no convincing mechanisms for accelerating particles to these energies. Interaction with the cosmic microwave background (CMB) constrains protons of $\sim 10^{20}$ eV to come from distances not greater than about 50 Mpc [2,3]. Similarly constrained are other primaries: heavier nuclei lose energy by photo-disintegration and pair production, and photons due to pair creation [4]. Furthermore, the flux of cosmic rays at these highest energies is very low (less than one event per km² per century per sr), so that their detailed study requires detectors covering large areas.

The Pierre Auger Observatory was designed for a high statistics, full sky study of cosmic rays at the highest energies [5]. It utilizes an array of surface water-Cherenkov detectors combined with air fluorescence telescopes, which together provide a powerful instrument for air shower reconstruction. Energy, direction and composition measurements are intended to illuminate the mysteries of the most energetic particles in nature.

On dark moonless nights, air fluorescence telescopes record the development of what is essentially the electromagnetic shower that results from the interaction of the primary particle with the upper atmosphere. The surface array measures the particle densities as the shower strikes the ground just beyond

Email address: ingo@cab.cnea.gov.ar (for the Pierre Auger Collaboration).
URL: www.auger.org.ar; www.auger.org (for the Pierre Auger Collaboration).

22 its maximum development. By recording the light produced by the developing
23 air shower, fluorescence telescopes can make a near calorimetric measurement
24 of the energy. This energy calibration can then be transferred to the surface
25 array with its nearly 100% duty factor and large event gathering power [6,7].
26 Moreover, independent measurements with the surface array and the fluores-
27 cence detectors alone have limitations that can be overcome by combining the
28 results of their measurements.

29 The water-Cherenkov detector was chosen for use in the surface array because
30 of its robustness and low cost. Furthermore, water-Cherenkov detectors exhibit
31 a rather uniform exposure up to large zenithal angles and are sensitive to
32 charged particles as well as to energetic photons which convert to pairs in
33 the water volume. Their use in surface arrays was proven to be successful in
34 previous experiments [8].

35 Each of the 1600 surface detector stations includes a 3.6 m diameter water
36 tank containing a sealed liner with a reflective inner surface. The liner contains
37 12 000 l of pure water. Cherenkov light produced by the passage of particles
38 through the water is collected by three nine-inch-diameter photomultiplier
39 tubes (PMTs) that are symmetrically distributed at a distance of 1.20 m
40 from the center of the tank and look downwards through windows of clear
41 polyethylene into the water. The surface detector station is self-contained. A
42 solar power system provides an average of 10 Watts for the PMTs and elec-
43 tronics package consisting of a processor, GPS receiver, radio transceiver and
44 power controller. The components of the surface detector station are shown
45 in Fig. 1.

46 In this paper we describe the design features and performance of the surface
47 detector hardware. This description includes the detector tanks, liners and
48 accessories and the pure water production, as well as the most relevant steps
49 for assembly and deployment of the surface detectors. We conclude with an
50 overview of the technical performance of the system. The electronics system
51 of the surface detectors will be described in a companion paper [9].

52 The Southern site of the Auger Observatory, now under construction in the
53 Province of Mendoza, Argentina, is over 85% completed. Active detectors have
54 been recording events in a stable operation mode since January 2004 [10].

55 **2 Design Considerations**

56 The low event rate of the highest energy cosmic rays requires an area large
57 enough to accumulate good statistics in a reasonable time. By covering an area
58 of 3000 km² at the Southern Site, the aperture achieved with the surface array

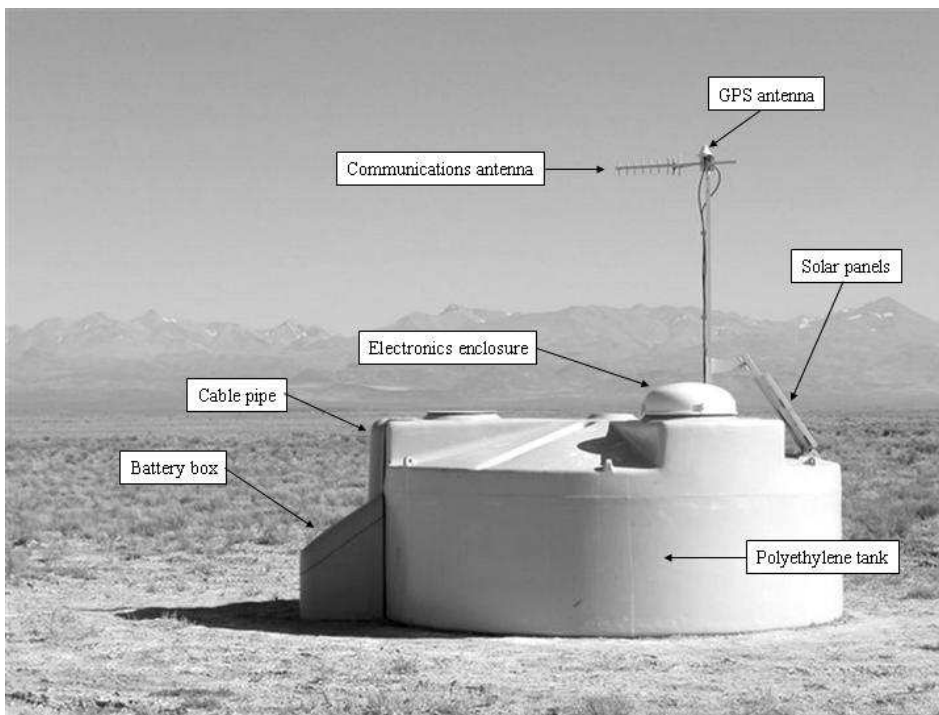


Fig. 1. A schematic view of a surface detector station in the field, showing its main components.

59 for zenith angles less than 60° will be $7350 \text{ km}^2 \text{ sr}$. By including events with
60 larger zenith angles, up to 80° , the aperture can be increased by $\sim 30\%$ [11].
61 The detection efficiency at the trigger level reaches 100% for energies above
62 $3 \times 10^{18} \text{ eV}$ [12]. This energy is determined from knowledge of the lateral distri-
63 bution of showers and the single detector trigger probability, without recourse
64 to Monte Carlo calculations. The spacing between the detector stations is the
65 result of a compromise between cost considerations and the energy threshold
66 (low enough to ensure a good overlap with existing data.) Other important
67 considerations are the need for sufficient sampling of the particle density away
68 from the shower core, and the need for shower front timing in several locations.
69 A minimum of five stations triggering at 10^{19} eV allows a maximum spacing
70 of 1500 m on a triangular grid. At this spacing, approximately 10 stations
71 are triggered by a nearly vertical shower with an energy of 10^{20} eV . At large
72 zenith angles the multiplicity of stations triggered increases and at $\sim 60^\circ$ it is
73 typically over 20. Differential GPS systems allow the determination of position
74 and altitude of the stations with an accuracy of less than 1 m, sufficient for a
75 good shower reconstruction.

76 For the installation of this array, the site is required to be flat for good wireless
77 communications. An altitude between 1000 and 1500 m above sea level is
78 required for optimal development of the shower in the atmosphere. A large
79 semi-desert area in the west of Argentina was chosen (35.0° to 35.3° S , 69.0°
80 to 69.4° W) [13] next to the city of Malargüe . The chosen site has an average
81 altitude of 1420 m, with detectors located at altitudes between 1340 m and
82 1610 m. The site has suitable infrastructure nearby as well as clear night
83 skies and minimal light pollution which enables good fluorescence detector
84 performance.

85 *2.1 Energy and Angular Resolution and Composition Determination*

86 The shower energy is obtained by determination of the signal density at a par-
87 ticular distance (typically 1000 m) from the shower axis. With the subset of
88 events that the Observatory detects in hybrid mode (simultaneous measure-
89 ment with both surface and fluorescence detectors), the nearly calorimetric
90 energy determination which is possible with the fluorescence data can be used
91 for an absolute calibration of the surface detector energy [6,7].

92 The signal densities measured with the surface detector array are affected
93 by fluctuations from different origins: statistical fluctuations in the measured
94 density, experimental uncertainties on the shower core position, incidence di-
95 rection, and large physical fluctuations in the shower longitudinal development
96 that lead to shower to shower fluctuations. The sampling fluctuations, which
97 are dominated by the muon content of the showers, are determined by the

98 sampling area of the detector. At distances of around 1000 m from the shower
99 core, the muon flux is of the order of $\sim 1 \text{ m}^{-2}$ at 10^{19} eV and corresponds
100 to roughly a half of the total signal, the other half being due to the electro-
101 magnetic component of the shower. Then, with a detector surface of 10 m^2
102 the sampling error in each detector is below 20%. For cylindrical detectors,
103 this corresponds to a diameter of 3.6 m. The statistical uncertainty (including
104 sampling and reconstruction fluctuations) in the determination of the signal
105 density at 1000 m from the shower core is of 10% RMS for events with an
106 energy of 5×10^{18} eV [14,15].

107 The direction of the primary is inferred from the relative arrival times of
108 the shower front at different surface detectors. A weighted minimization is
109 applied to fit the station triggering times to a parabolic shower front [16]. A
110 refined determination of the position of the shower core is obtained by fitting
111 the station signal densities to the expected lateral distribution. The angular
112 resolution improves rapidly with energy and zenith angle because of the greater
113 number of triggered stations. For the surface array alone, the angular precision
114 is better than 1° for energies larger than $\sim 10^{19}$ eV [17,18].

115 The height of the water-Cherenkov detector is chosen to get a clear muon
116 signal [19] and optimize the separation of the muon and electromagnetic con-
117 tributions to the signal. A vertical height of 1.2 m of water is sufficient to
118 absorb 85% of the incident electromagnetic shower energy at core distances
119 larger than 100 m, and gives a signal proportional to the energy of the elec-
120 tromagnetic component. Muons passing through the tank generate a signal
121 proportional to their geometric path length inside the detector and rather in-
122 dependent of their zenith angle and position. Each PMT collects in excess of
123 90 photoelectrons for each vertical muon [20].

124 *2.2 Physical and Environmental Requirements*

125 The Observatory will have an operating lifetime of 20 years and must be de-
126 signed to survive the expected conditions at the site. The temperature ranges
127 from -15°C to 50° with large diurnal variation. The outdoor location ex-
128 poses the detectors to intense solar ultraviolet radiation and wind of up to
129 160 km h^{-1} . The detectors must be resistant to floods, rain, snow, dust, wind-
130 blown sand and 2.5 cm diameter hail. Material selection is important because
131 the local soils contain salts which can be corrosive to some materials. Mod-
132 est seismic activity should not damage the detector units. The detector tanks
133 must be robust and able to support a heavy person on top of the tank as well
134 as to resist the action of insects, rodents and grazing animals.

135 The ground on which each detector station is placed must be leveled to prevent

136 deformation of the tank and the area around the detector must be cleared of
137 heavy vegetation to avoid damage from bush fires.

138 *2.3 Design, Development and Production Control*

139 Each stage in the design, development and production of the surface detector
140 station was marked by an appropriate technical review. Subsequent to the
141 preliminary design review, 32 prototype detectors were built, deployed with
142 standard spacing and operated in a small Engineering Array [21]. Every design
143 feature of the detectors, the communications systems and data acquisition was
144 tested during the two years allocated to the Engineering Array. Refinements
145 resulting from this period were incorporated into the baseline design and sub-
146 jected to a critical design review. A pre-production run of 100 detectors was
147 then built to qualify the production process. Production readiness reviews
148 initiated large scale component production. Assembly and deployment pro-
149 cedures and associated quality assurance steps were also qualified during the
150 Engineering Array and pre-production phases.

151 Individual assembly steps are documented in controlled written procedures,
152 which are also used for training and guidance of the staff. A database was
153 developed for the traceability of detector components and the results of the
154 tests performed on them.

155 **3 The Tank System**

156 *3.1 Tanks*

157 The water-Cherenkov detectors have a cylindrical shape for the water volume,
158 which is the simplest and least expensive to manufacture. The top of the
159 tank is rather complex in order to provide rigidity both for mounting external
160 components such as the solar panels and for people standing on top of it, and
161 to provide space inside the tank for the photomultiplier assemblies and cabling.
162 The tanks do not exceed 1.6 m in height so that they can be shipped over the
163 roads within transportation regulations. The beige tank color is selected to
164 blend in with the natural background of the site. Although the tank liner and
165 photomultiplier assemblies are designed for opacity to keep any external light
166 away from the PMTs, the tank is totally opaque to provide redundancy.

167 For the manufacture of the surface detector tanks, the technique of rotational
168 molding (also called “rotomolding”) of high-density polyethylene was chosen

169 for its low cost, tank uniformity and because polyethylene meets the require-
170 ments of robustness against the environmental elements.

171 In the rotomolding process, a predetermined amount of light beige powdered
172 polyethylene is deposited inside a steel or stainless steel mold. The inside
173 of the mold has the shape desired for the outside of the tank. The mold is
174 closed and rotated about two axes simultaneously inside a 300°C oven. The
175 beige powdered polyethylene melts and forms a coating on the inside surface
176 of the mold. Heating and rotation continues until all the powder has been
177 deposited on the surface of the mold. The rotation is briefly stopped and a
178 predetermined amount of black powdered polyethylene is put inside the mold,
179 which is immediately re-closed and the rotation in the oven continues until all
180 of this powder has been deposited on the surface. Then the mold is removed
181 from the oven and cooled while the rotation continues. Finally, the mold is
182 opened and the tank removed.

183 This process, which requires between four and six hours, produces tanks with
184 a light-beige outer layer of 1/3 of the thickness, and an opaque black inner
185 layer guaranteeing that the tank itself will be opaque. Care in the manufac-
186 turing process results in a nearly uniform wall thickness of the desired (13
187 ± 3) mm and minimal warping. The nominal weight of each tank is 530 kg,
188 varying slightly with each manufacturer. Four companies produced tanks for
189 this project.

190 Lugs are molded into the tank for lifting it and for supporting the solar panels.
191 The solar panel bracket lugs are drilled to the correct diameter after molding
192 and access hatches are cut into the tank.

193 The 20-year lifetime of the tanks under outdoor conditions is a challenging
194 specification. However, discussions with consultants and experts in the field
195 convinced us that this can be achieved using high-quality polyethylene resins.
196 To greatly reduce damage due to ultraviolet exposure, modern polyethylenes
197 contain hindered amine light stabilizers (HALS). In addition, ultraviolet light
198 is absorbed by titanium dioxide found in the beige pigment of the outer layer
199 and by the 1% carbon black pigment of the inner layer. The polyethylene
200 resins used for tank production are prepared in two stages. The first one is the
201 manufacture of the base resin by polymerizing selected alkenes with suitable
202 catalysts. This stage of manufacture also includes the addition of the light
203 stabilizers and anti-oxidants. The character and quality of the resin are de-
204 termined in this stage. The second stage is “compounding”. The polyethylene
205 resin thus manufactured is melted and the required pigments are extruded into
206 the resin in such a way that they mix very finely with the base polyethylene.
207 Other additives, like HALS and antioxidants, can be mixed in at this stage as
208 well. Then the resin is cooled and ground into a powder ready for the molding
209 process.

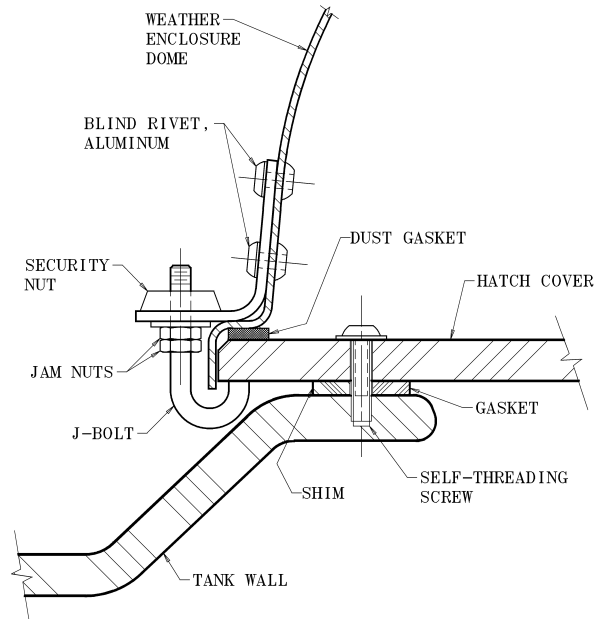


Fig. 2. Details of the hatchcover sealing system and the electronics weather enclosure dome attachment

210 Creep over the 20 years lifetime might also cause the tank to deform. Creep
 211 measurements of samples of our resins and extensive finite element analysis
 212 indicate that creep would not be a problem. Indeed, no evidence of either creep
 213 distortion or ultraviolet degradation have been observed in any tank, some of
 214 which have been in service for over five years.

215 3.2 Hatch Covers and Electronics Enclosure

216 As can be seen in Figs. 1 and 2, the tank hatches are elevated, to prevent
 217 rainwater from accumulating around the hatchcover and leaking into the tank.

218 The hatchcover assemblies for the three hatch openings (one large, 560 mm
 219 diameter, and two small, 450 mm diameter) consist of hatchcovers, gaskets,
 220 shims between the tank and hatchcover, and fastening screws. They seal and
 221 protect the tank contents, keeping out light, water and dust. They are easily
 222 removable for access to the tank contents. The large hatchcover is the mount-
 223 ing location for the electronics and has penetrations for cable feed-throughs.

224 The hatchcovers are of similar material to the tank itself so that stresses in the
 225 attaching screws are minimized. Hatchcovers are machined from 12.7 mm high-
 226 density, two-layer polyethylene (HDPE) sheets with beige on the outer side
 227 and opaque black on the inner side. The shape of the hatchcover is a simple
 228 disk with 24 equally spaced holes around the outer edge for the attaching

229 screws.

230 The purpose of the shim is to control the spacing between the tank top and the
231 hatchcover at the location of the gasket, to limit its amount of compression.
232 The shims (polyethylene) and gaskets (foam polyurethane) are bonded to the
233 hatchcover using 3M 9472 acrylic adhesive transfer tape¹ which is particularly
234 good at bonding to low surface energy materials, including polyethylene.

235 The hatchcovers are attached to the tanks using self threading screws designed
236 for thermoplastics, identified as Plastite 48-2. The 5.3 mm diameter screws are
237 made from stainless steel and have a tamper-resistant (pin-in-head) Torx head
238 for increased security.

239 The detector electronics enclosure is mounted on the large hatchcover and
240 protected by a weather enclosure, a dome that provides rain and dust pro-
241 tection and the outer security layer. The dome can be seen in Fig. 1. The
242 dome itself is spun from 2.3 mm soft aluminum. A foam polyurethane dust
243 gasket is installed inside the lower lip so that it compresses against the large
244 hatchcover. The dome is painted beige to match the color of the tank. The
245 hold-down system for the weather enclosure consists of a bracket riveted to
246 the dome, a J-bolt which engages the large hatchcover, two jam-nuts and one
247 security nut, which can be opened only with a special tool.

248 *3.3 Battery Box System*

249 Attached to the surface detector station is a rotational molded polyethylene
250 box containing the batteries and charge regulator for the solar power system.
251 The battery box, visible in Fig. 1, is placed on the southern side of the tank,
252 where the tank protects it from direct sunlight to keep the temperature low
253 and thus increase the lifetime of the batteries. A polyethylene plate is screwed
254 to the bottom of the box and extends below the tank to anchor the box,
255 deterring theft or displacement by large animals. The box has a rounded back
256 with radius of curvature equal to the tank radius to fit close to the tank. The
257 corners of the box are rounded to discourage rubbing by cows. The interior of
258 the box is lined with 50 mm polystyrene foam sheets as thermal insulation.
259 The top of the box has a slope to deter its use as a step to get on the tank.
260 The lid is held on with security-head screws. A protective cover is mounted
261 to the tank to shield the power system cables that run from the inside of the
262 tank, above the water level, to the interior of the battery box.

¹ 3M, St. Paul, Minnesota, U.S.A., www.3m.com

263 4 Solar Power System

264 4.1 Solar panels and batteries

265 Power for the electronics is provided by a solar photovoltaic system. The power
266 system provides the required 10 W average power. A 24-V system has been
267 selected for efficient power conversion for the electronics.

268 Using the available insolation data for the Auger site, it was found that a
269 suitable power system can be obtained with two 55 Wp panels² and two
270 105 Ampere-hour (Ah), 12 V batteries. Power is expected to be available over
271 99% of the time. Even if after long-term operation the capacities of the solar
272 panels and batteries are degraded to 40 Wp and 80 Ah, respectively, power
273 would be available 97.8% of the time.

274 The batteries³ selected for the project are a new type of lead acid battery
275 designed for solar power applications. They have a selectively permeable mem-
276 brane and do not require maintenance. Other lead-acid battery technologies
277 are being considered for replacement batteries as these wear out.

278 The charge controller⁴ was selected for robust design and construction, to
279 maximize the lifetime expectations. An encapsulated, epoxy potted model
280 with robust surge protection was found in the solar power market. The con-
281 troller is pulse width modulated and operates by applying pulses of current of
282 varying width to the batteries, as their state of charge varies with battery volt-
283 age and temperature. This is considered to be the best method of charging for
284 maintaining battery efficiency and lifetime. There have been no observations
285 of electronics interference arising from the charge controller.

286 4.2 Solar Panel Support Brackets and Masts

287 The solar panel bracket supports the solar panels and includes the mast that
288 supports the communications antenna and the GPS antenna. To optimize
289 light collection in winter time, the solar panels are installed such that they
290 face North, at an inclination of 55 degrees with respect to the upward-looking
291 position. The bracket system is designed to withstand 160 km h⁻¹ winds.

² Wp is a unit expressed in watts for solar panel output with a standard solar irradiation applied.

³ Model 12MC105, Acumuladores Moura S.A., Brazil, www.moura.com.br

⁴ SunSaver SS-10-24V, Morningstar Corporation, U.S.A.,
www.morningstarcorp.com

292 The brackets are built using aluminum 38 mm square tubing with aluminum
293 blind rivets, and the aluminum alloys used were selected for good corrosion
294 resistance. The brackets are prepared by cutting, drilling and riveting most
295 of the assembly in a factory. A few of the rivet holes are not drilled until the
296 bracket is test-fitted to the tank, so that the variability in the dimensions
297 from tank to tank is compensated for. The assembly of the solar panels to the
298 brackets and of the brackets to the tank is completed before the detectors are
299 taken out into the field, but the brackets are left in a collapsed configuration
300 for ease of transportation. When the detector is in its final position the panels
301 and mast are raised and locked in place by a single bolt.

302 *4.3 Power Cabling*

303 By mounting the electronics directly on the hatchcover, the length of cables
304 and the number of connections and feed-throughs are minimized. The power
305 cables run from the solar panels to the electronics enclosure and from there
306 through the interior of the tank to the battery box. They penetrate the large
307 hatchcover and the tank with light- and water-tight cable feedthroughs. The
308 only cables exposed to the outside world are the two antenna cables and the
309 solar power cable coming from the bracket assembly and entering the electron-
310 ics enclosure. They are UV protected for outside use. Heavy gauge wiring was
311 selected for robustness rather than for electrical resistance considerations.

312 Sensor cables are installed with the power cables. Voltage of the individual
313 batteries, their charge and discharge current as well as the temperatures of
314 the batteries and the bases of the PMTs are monitored and registered in 6-
315 minute intervals. The monitoring of the batteries is also required as the tank
316 power control board is designed with the capability of setting the local station
317 in hibernation mode if the voltage drops too low after many days without
318 sunshine. After a period of prolonged cloudiness, all stations of the array can
319 be shut down simultaneously rather than shutting down individual stations,
320 minimizing recovery times and maximizing data integrity. Power system con-
321 nectors are automotive grade, gold-plated for long durability in the harsh field
322 conditions.

323 A grounding rod is driven into the ground at the opening between the bat-
324 tery box and the tank and connected to the negative terminal to provide the
325 electronics system grounding.

326 5 Liners

327 5.1 Development and Design

328 Tank liners are right circular cylinders made of a flexible plastic material
329 conforming approximately to the inside surface of the tanks. The liners fulfill
330 three functions: they enclose the water volume, preventing contamination or
331 the loss of water and providing a barrier against any light that enters the
332 closed tank; they diffusively reflect light traversing the water; and they provide
333 optical access to the water volume for the PMTs, such that PMTs can be
334 replaced without exposing the water to the environment.

335 Three dome windows and five fill ports with screw caps are hermetically sealed
336 to the liner. The window assemblies allow for the mounting of the PMTs. The
337 fill ports allow for filling and venting the tank, as well as providing a window
338 for an LED flasher used for initial testing.

339 Although the tanks provide the primary light barrier for external light sources,
340 it is necessary that the liners be completely opaque to act as a secondary
341 protection against small light leaks. Initial tests were performed to ensure
342 that the laminate and the seals are completely opaque against single-photon
343 level light transmission, i.e., a 0% light transmission for light of wavelengths
344 between 300 and 700 nm, as measured by counting single-photon detection
345 rates.

346 Although the mass of water moderates temperature fluctuations, the temper-
347 ature range to which the liner is exposed is from nearly -10°C to $+50^{\circ}\text{C}$. Up to
348 10 cm of ice could form at the upper surface or sides of the water volume. The
349 liner is designed to be sufficiently strong and flexible that it is not damaged
350 by such ice formation. Ice is prevented from forming near the PMT windows
351 by mounting insulating rings of polystyrene foam. Strength and flexibility are
352 also required to withstand the formation of waves up to 15 cm high on the
353 surface of the water produced by eventual seismic activity. The Observatory
354 is located in an area rated for moderate seismic activity and the detector was
355 designed to resist damage from such activity.

356 Liner materials require strength, opacity to external light, diffuse reflectivity
357 of inner surface, sealability, resistance to chemicals from the environment and
358 to biological activity and minimal extractables from the material which might
359 contaminate the water volume enclosed.

360 The liners are produced from a laminate composed of an opaque three-layer
361 co-extruded low-density polyethylene (LDPE) film bonded to a 5.6 mils thick

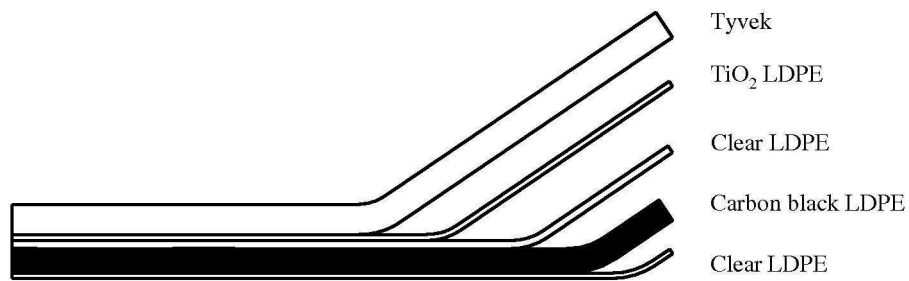


Fig. 3. A sketch of the laminate, showing the outer Tyvek[®] layer, the medium TiO₂ LDPE layer and the 3-layer with clear LDPE, LDPE with carbon-black and clear LDPE.

362 layer of Dupont Tyvek[®] 1025-BL⁵ by a layer of Titanium-dioxide pigmented
363 LDPE of 1.1 mils thickness (see Fig. 3). The three-layer co-extruded film con-
364 sists of a 4.5 mils thick carbon black loaded LDPE formulated to be opaque to
365 single photons, sandwiched between layers of clear LDPE to prevent any car-
366 bon black from migrating into the water volume. The LDPE was metallocene
367 catalized linear low-density polyethylene (LLDPE) with excellent strength
368 and flexibility. Tyvek[®] 1025-BL was chosen as the reflective layer due to its
369 strength and excellent diffuse reflectivity for Cherenkov light in the near ultra-
370 violet [22,23]. Tyvek[®] 1025-BL is an untreated polyolefin non-woven material,
371 which minimizes the chemicals available to leach into the water volume. It is
372 the thinnest of the “biological grade” Tyvek[®] commercially available, which
373 simplifies the bonding processes used in manufacturing liners.

374 Polyolefin film has a strong tendency to pick up electrostatic charge when un-
375 rolled or pulled over a surface and even in a very clean assembly environment
376 would collect significant dust during the hours involved in liner assembly. The
377 method for controlling contamination of the liners centers on minimizing food
378 sources for microbes by eliminating hair and skin contact with the lamination
379 and working in a reasonably clean environment. Although the Auger lamina-
380 tion is not produced in a “clean room” environment, the extruders, lamination
381 machines and slitting machines are all cleaned prior to production of the Auger
382 lamination, and hair restraints and gloves are worn during all handling of the
383 film.

384 5.2 Assembly and Testing

385 Liners are assembled by first manufacturing three separate sections of laminate
386 and then sealing them together. The separate sections are the bottom, side
387 strip, and top. The liner top is the most complex section since it includes
388 the PMT and LED windows and fill/vent ports. Seals are made by welding
389 the layers together under pressure with custom designed impulse heat seal
390 machines. The liner tops were assembled using the same cleanliness procedures
391 as for laminate manufacture mentioned above. Final liner assemblies were done
392 in a class 100 000 clean room specially set up for this project.

393 All liners were tested for leaks and flaws, and any defects were repaired before
394 packing and shipping to the site. The same tests were repeated at the assembly
395 site prior to installation.

396 For testing, the liner is inflated to a pressure of 20 millibar over atmospheric
397 pressure, see Fig. 4. Then all the seals are tested using a soap bubble solution,

⁵ E.I. du Pont de Nemours and Co., Wilmington, Delaware, U.S.A.,
www.dupont.com

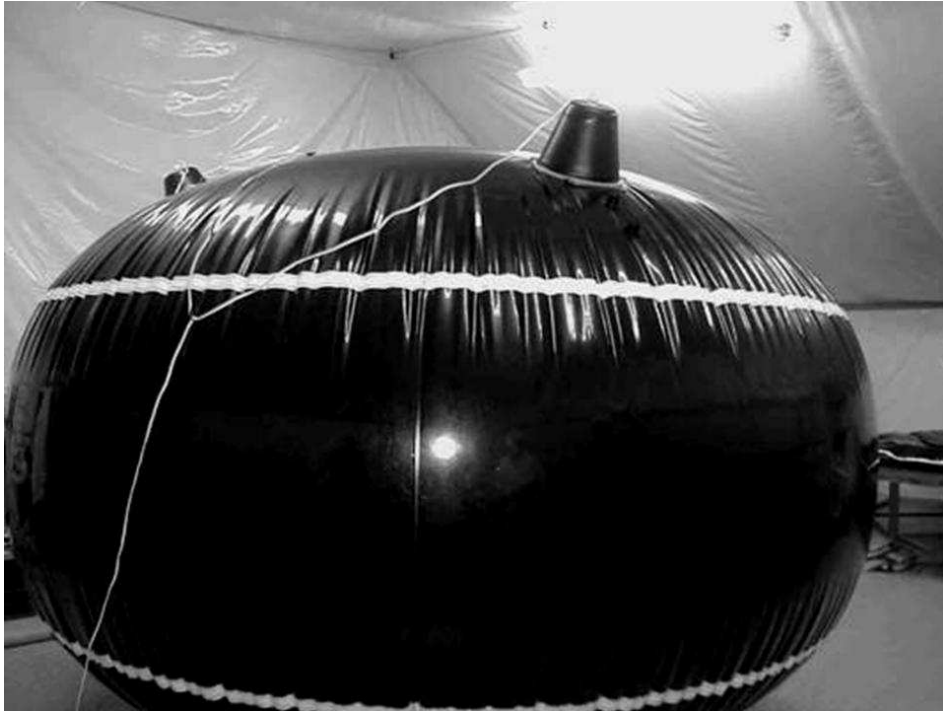


Fig. 4. An inflated liner during testing.

398 looking for visible signs of bubbling. The liner is then examined in a darkened
399 room with bright lights covering the window ports such that they only illu-
400 minate the interior of the liner. Any visible light leaking out from the liner
401 indicates a fault requiring repair. The testing procedures described above were
402 determined to be sensitive to leaks smaller than those which could cause a loss
403 of 10% of the detector volume in 20 years.

404 *5.3 Dome Assembly and PMT Enclosure*

405 The PMT enclosures have been designed to allow the PMT to collect Cherenkov
406 light from the water detector volume while providing for a cover to shield the
407 PMT from external light and protecting it from the external environment (see
408 Fig. 5).

409 The foundation of the PMT assembly is an annular, LLDPE flange that is
410 heat-sealed directly to a hole in the top of the liner using a custom circular
411 heat impulse welder. The window through which the PMT views the water
412 is made of UV-transparent LLDPE. The windows are vacuum formed to fit
413 approximately the nominal PMT face. The window is heat sealed to the flange.
414 Using heat seals rather than any adhesive insures that the only material in
415 contact with the water is polyethylene. The PMT is protected on the top
416 from light by an injection-molded ABS plastic cover called the “fez”. For

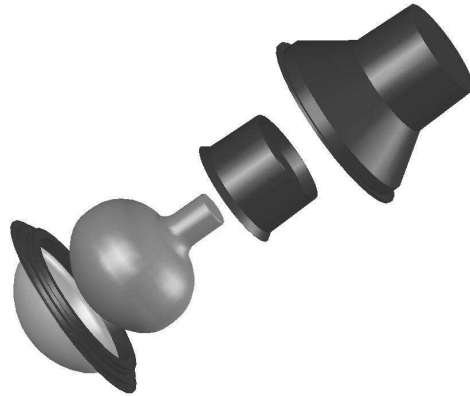


Fig. 5. Mechanical housing for the PMT (top to bottom): Outer ABS plastic housing; insulating plug affixed to the PMT neck that centers the PMT and sets the distance of the PMT face to the window; PMT; flange to which the housing is glued with a room- temperature RTV; UV-transparent window which is fixed to the PMT using a UV-transparent optical coupling.

417 installation the PMT is indexed with respect to the fez using an internal
418 polystyrene foam collar that is bonded to the PMT neck. The variance in
419 the PMT face shape results in a few millimeters uncertainty on the space
420 between the window and the PMT face, and that space is filled with 150 ml of
421 the silicone optical compound GE6136 RTV⁶. Without the optical coupling
422 approximately half the light from the tank is lost due to total internal reflection
423 and direct reflection from the interfaces. The fez, with PMT in place, is sealed
424 to the flange using black GE 123 RTV⁶ at the time that the optical seal is
425 made. The fez has four ports. One port is a light-tight air vent to prevent
426 pressure buildup due to temperature changes. The other three ports are for
427 cable feed-throughs. These are custom molded two-piece parts (identical left
428 and right parts) that clip around the cables and clip to flat annular regions on
429 the fez. There are similar feed-throughs to pass cables through the bottom of
430 the hatch cover into the electronics enclosure. Finally there are two annular
431 polystyrene foam insulation pieces that fit inside the fez to prevent ice buildup
432 near the PMT. One insulation piece is the same one that fits on the PMT neck
433 to fix its position with respect to the fez. The other fits at about water level
434 and fills the space between the inside of the flange and the top of the bulb of
435 the PMT glass. Tests show that ice will form in extreme years on the water
436 surface, but with the insulation in place it will not stress the optical coupling
437 or the PMT itself.

⁶ General Electric Company, U.S.A., www.gesilicones.com

438 6 Water

439 6.1 Water Quality Specification

440 Each surface detector contains 12 000 l of ultra-pure water. The high water
441 purity is required for two purposes: to achieve the lowest possible attenuation
442 for UV Cherenkov light, and to guarantee stability of the water during the
443 20 years of operation of the detectors.

444 For these reasons, the detector water needs to be deionized and completely
445 free of microorganisms and nutrients. After consulting experts in pure water
446 production, it was established that the best achievable water quality requires
447 a water treatment that gives an output water of resistivity above 15 M Ω -cm.

448 The production rate of the water plant has to be high enough to ensure that
449 it can provide water to the detectors at the same rate as they are deployed.
450 This requirement corresponds to up to 36 000 l/day, which would allow us to
451 fill up to 90 detectors per month.

452 6.2 Water Production

453 The pure water required for the surface detectors is produced at a plant owned
454 and operated by the Auger Observatory and installed at the Central Campus
455 in Malargüe.

456 Water is provided both from a local well at 80 m depth and from the city of
457 Malargüe water network and pumped to a cistern with 60 m³ capacity where
458 it is chlorinated and stored. The water plant is fed from this cistern. As the
459 quality of the city water is considerably better than the underground water
460 but more expensive, the admixture allows an increased production rate and
461 reduced contamination in the effluents at the lowest cost.

462 The water purification follows four stages:

- 463 (1) Pre-processing:
- 464 • Prefiltering, to eliminate particles greater than 40 μm .
 - 465 • Softening with a resin bed for strong cationic exchange, with regenera-
466 tion by sodium chloride, to eliminate Ca⁺⁺, Mg⁺⁺ and Fe ions.
 - 467 • Addition of antiscaling solution, to avoid deposit of silicates on the reverse
468 osmosis membranes (see below).
 - 469 • Addition of chlorine reducer to eliminate active chlorine.
 - 470 • Microfiltering with two pairs of polypropylene microfilters to eliminate

- 471 particles greater than 5 μm .
- 472 • Ultraviolet disinfection with a 254-nm UV unit (64 W power), to elim-
473 inate microorganisms from the water.
- 474 (2) Reverse osmosis: A high-pressure centrifugal pump pressurizes the wa-
475 ter and pumps it to the reverse osmosis unit, consisting of two modules
476 in parallel with 4 membranes each and, in series at their output, a third
477 module with 4 membranes. Maximum input flow is 4500 l/h, with a max-
478 imum output of 2800 l/h. The output water resistivity is $\sim 100 \text{ k}\Omega\text{-cm}$.
- 479 (3) Ultraviolet purification: an ultraviolet source of 185 nm eliminates micro-
480 biological residues and removes Total Organic Carbon (TOC).
- 481 (4) Continuous Electrodeionization (EDI): To achieve the required final water
482 quality (resistivity above $15 \text{ M}\Omega\text{-cm}$), the product of the reverse osmosis
483 process is fed to an EDI unit⁷, which consists of a set of membranes with
484 cationic and anionic transfer. The production capacity of this unit is up
485 to 3400 l/h.

486 The high-purity output water is stored in a 50 000 l storage tank. A recircu-
487 lation system, which also permits quality improvement through a mixed resin
488 bed and UV treatment (254 nm, 151 W), can recirculate up to 5 500 l/h. The
489 pumping system of this recirculation is also used to fill the transport tank.

490 The water plant is fully automated. Instruments monitor the working param-
491 eters of the water plant: a chlorine monitor at the entrance of the reverse
492 osmosis membranes, pressure gauges, flux gauges, flow meters and resistivity
493 meters. A programmable logical controller (PLC) records the relevant produc-
494 tion parameters.

495 6.3 Water Testing and Handling

496 The two most relevant parameters that give information about water quality
497 are its resistivity and biological activity. Resistivity can be measured contin-
498 uously at the output of the water plant and in the storage tank with the
499 instruments incorporated at the water plant. Resistivity of the water in the
500 transport tank and in the detectors is determined with hand-held conductivity
501 meters. Although the water resistivity degrades during transportation, prob-
502 ably due to absorption of carbon dioxide, tanks in the production phase are
503 filled with water of 8 to $10 \text{ M}\Omega\text{-cm}$. During the initial phases of the project,
504 Engineering Array tanks were filled with water of less than $1 \text{ M}\Omega\text{-cm}$ quality
505 and they worked as required for nearly 4 years [21].

506 The TOC, i.e., potential nutrients for bacteria, is removed by the short wave-

⁷ Model E-Cell MK-1 PHARMA, General Electric Company, U.S.A.,
www.gewater.com

507 length UV exposure followed by deionization. The plant manufacturer specifies
508 that 10 ppb should be achieved. It is not feasible to measure TOC in the tanks
509 deployed in the field with the required accuracy, so TOC was only measured
510 a few times at the output of the water plant, yielding values below 100 ppb.

511 To determine the biological activity in the water, samples are taken periodi-
512 cally from the storage tank, the transport tank and the detectors themselves.
513 These samples are kept in a sterile container and sent to a biochemists' lab-
514 oratory to perform the corresponding analysis and search for aerobe meso-
515 phylls, coliforms, faecal coliforms, coliforms in Koser citrate, yeasts and fungi
516 in Agar Saboreaud medium. In most of the cases, no biological activity has
517 been found. Some isolated tanks showed contamination with low quantities of
518 aerobe mesophylls, identified as being of the genus "Serratia", which might
519 originate from contamination during sampling or during sample transporta-
520 tion. In all cases, the initially detected bacterial contamination was low (below
521 2000 colony forming bacteria per ml) and these tanks were monitored period-
522 ically and in no case could a large or steady increase in bacterial activity be
523 detected.

524 6.4 Long-Term Stability

525 The long-term trends in water quality are tracked using the on-line tank cal-
526 ibration and monitoring system that is active for every station and updates
527 every four hours [20]. In this application, the time structure of the collected
528 Cherenkov light produced by through-going muons is recorded to measure the
529 water purity indirectly [24]. Use of the calibration and monitoring system has
530 the advantage that every station in the array can be followed and the great
531 quantity of data collected allows some predictive power even if the measure-
532 ment lacks the directness of water sampling.

533 The charge registered in the fast analog-to-digital converter from single muons
534 rises rapidly, peaks, and then decreases exponentially. The decay time depends
535 on the rate of Cherenkov light absorption and on the reflectivity of the interior
536 of the liner. Measuring the time constant quantifies the amount of Cherenkov
537 light that is absorbed in a way that is largely unrelated to the absolute photo-
538 electron count. An absolute photon count depends on more than just the
539 amount of absorption in a station. Although it is possible to fit the muon
540 traces directly and obtain the time constant, this method is dependent on
541 the precise details of the fitting procedure. For this reason Q_{VEM} (the total
542 charge deposit by a vertical muon) divided by I_{VEM} (the signal maximum for
543 a vertical muon) is used as a substitute for the actual time constant. That
544 ratio can then be examined as a function of time to search for trends that
545 have time scales in the range of a few months to several years.

546 Application of this technique allowed us to observe a decline by 10% in the
547 Q_{VEM}/I_{VEM} ratio in the first several months after deployment, at which time
548 it reaches an equilibrium. The origin of this behaviour is still under inves-
549 tigation. After this the water quality is nearly constant with a small annual
550 oscillation of less than 1% in the Q_{VEM}/I_{VEM} ratio, linked to seasonal changes.

551 7 Detector Assembly and Deployment

552 7.1 Detector Assembly

553 The assembly of the surface detector stations is done in the Assembly Building
554 located at the Central Campus of the Observatory in Malargüe. The differ-
555 ent components are received and assembled into a complete detector in this
556 building, which provides workspace for eight detectors at a time.

557 When received, tanks are unloaded and inspected. Using a template, holes are
558 drilled to guide the hatchcover screws and the hatches are closed to keep water
559 and dirt out of the tank during outdoor storage. Dimensional measurements,
560 including ultrasonic measurements of the tank wall thickness, are performed
561 to ensure tank quality. After cleaning, the tank interior is checked for imper-
562 fections that could damage the liner. Holes for venting, water drain and cable
563 feed-throughs are drilled into the tank, cables are passed through the interior
564 of the tank and the liner is inserted and inflated with filtered air. PMTs are
565 installed and glued to the liner window domes using optical RTV. Fezzes are
566 mounted over the PMTs to ensure a light-tight seal. The remaining items are
567 mounted to the tank: the half-pipe to protect the cables running outside the
568 tank, the solar panel brackets with solar panels and the electronics enclosure
569 dome. The liner is kept inflated with air for safe transportation to the field,
570 and foam pads are inserted between the PMT fezzes and the hatchcovers to
571 provide cushioning of PMTs during transportation. Six full time technicians,
572 one foreman and an administrative assistant (for data entry, inventory and
573 parts receiving and management) can assemble eight tanks every two days.
574 This includes the assembly of the solar panel brackets and the preparation of
575 the battery boxes. PMTs are tested in the Assembly Building after installa-
576 tion, and serial numbers of the main detector parts are recorded and entered
577 into the parts management database.

578 Detector deployment involves survey and site preparation, delivery of the de-
579 tector units to their prepared locations, delivery of water and installation of
580 the components necessary to complete the detector. The main challenge for
581 deployment is transportation over difficult and variable road conditions, par-
582 ticularly with heavy loads of water. Access to detector locations is affected by

583 seasonal and daily weather conditions.

584 *7.2 Site Survey and Preparation*

585 Prior to detector deployment, the ground for each surface detector location is
586 prepared following these steps:

- 587 • A contract surveyor marks the location where each detector is to be deployed
588 with two stakes oriented north-south at a distance of roughly 10 m from each
589 other. The surveyor provides the Project with information on the positioning
590 of both stakes (including altitude) with centimeter precision, as well as
591 information on ground conditions.
- 592 • A circular area of 6 m radius is cleared of vegetation. At locations with pam-
593 pas grass (“cortadera”) or heavy brush, the circular cleared area is increased
594 to 10 m radius to reduce the seasonal fire hazard. Local environmental reg-
595 ulations and procedures are observed.
- 596 • A central circular area of 2.5 m radius is prepared by clearing it of stones,
597 roots and other sharp objects and irregularities to avoid damage to the tank
598 bottom. The ground is leveled to within 3 cm to avoid overloading the walls
599 of the detector tank and to provide a uniform water depth and PMT height.

600 The aim was to place all of the detectors on a hexagonal grid of 1500 m
601 spacing. However, for practical reasons, deviations from this ideal have been
602 inevitable although the median location is within 12 m of the optimum po-
603 sition. Only 4% of the detector positions are more than 50 m away from the
604 ideal location, with 0.4% of the detectors being displaced more than 100 m.
605 These large displacements (which have little impact on reconstruction accu-
606 racy) were necessary because of a cultivated area, a riverbed or a swamped
607 and inaccessible area.

608 *7.3 Deployment*

609 The deployment procedure starts with loading assembled tanks and transport-
610 ing them to a staging area at the site. Tank transport to the staging area is
611 done with flatbed tractor-trailer trucks carrying four tanks at a time. Staging
612 areas are selected to be approximately equidistant from the four deployment
613 locations and in an area where the truck transporting the tanks can easily
614 maneuver. An escort vehicle carries other components for deployment.

615 Loading at the Assembly Building is done with a forklift truck. All tank lifting
616 is performed using the lifting lugs molded into the top of the tanks along with
617 clevises and straps. Unloading and further transportation at the site requires

618 a truck capable of carrying a single tank and equipped with a hydraulic crane.
619 Such trucks are commonly used for transporting bricks, drywall, roofing ma-
620 terials and other construction supplies. While being unloaded and positioned,
621 the tank is oriented such that the solar panel will face north (5° tolerance) as
622 determined with a compass. Once the tank is positioned, the battery box is
623 installed at the south side of the tank and batteries and charge regulator are
624 installed and connected.

625 Water is delivered to the detector as discussed in the following section. During
626 water filling, the water delivery team installs the communications antenna kit
627 and the GPS antenna and mounts them to the mast.

628 Finally, installation of the electronics kit is performed by a team of two elec-
629 tronics technicians. The electronics for the detector station are tested and the
630 detector is commissioned. Contact via a mobile radio system to a data ac-
631 quisition technician at the Central Campus allows the deployment technician
632 to check that the detector is performing correctly and sending triggers to the
633 central data acquisition system at the Central Campus before leaving the field.
634 At this stage the detector is fully integrated into the data taking system.

635 7.4 *Water Delivery*

636 Water is delivered to each detector tank (12 000 l) in one filling, with a sin-
637 gle hose connection. Only a single connection is used in an effort to prevent
638 contamination by bacteria and/or potential nutrients.

639 A water delivery system is composed of two 12 500 l tanks, one mounted on
640 the back of a truck and one mounted on a trailer. Each tank has an electrically
641 powered pump, a gasoline powered generator, hoses, connections and acces-
642 sories. The trailer is pulled by the truck on easy access roads and tracks. To
643 access the more difficult areas, the trailer or the truck are pulled by a large
644 front-end loader. The front-end loader is also used to even out irregular roads
645 and to compact the ground in wet areas.

646 The transport tank system has the following characteristics:

- 647 • The first transport tank that was acquired for water delivery was made of
648 fiberglass-reinforced polyester resin with food-grade protective coatings on
649 the inside. The maximum allowable working differential pressure of the tank
650 is 100 cm of water. For full scale deployment, three additional tanks were
651 purchased, made of stainless steel (AISI 304 with 2-b sanitary finishing) as
652 this is more robust to damage in the harsh field conditions and can be kept
653 clean more easily. Two of these tanks were mounted on trucks and two on
654 trailers.

- 655 ● A 0.2 μm bacteriological filter is connected to the air inlet of the tank to
656 filter the air that is sucked into the transport tank as the water is pumped
657 out. A valve is installed below the filter, to ensure that the water cannot
658 splash the filter during truck movements because the filter has a very high
659 pressure drop when wet. The valve is opened when the tank is being emptied
660 to allow inflow of air.
- 661 ● Each tank has a manway to allow access for cleaning. A pressure relief valve
662 is installed at the manway to avoid damage to the tank by overpressure
663 during filling.
- 664 ● There is a transparent plastic window on the tank for direct visual inspec-
665 tion.
- 666 ● A 50 mm hose and associated valves are installed to transfer the water
667 from the transport tank to the detector. The end of the hose is connected
668 to a bayonet that has a valve to regulate water flow and a freely rotating
669 cap that can be screwed to the liner opening. During transportation, the
670 bayonet is protected with a stainless steel scabbard which can be screwed
671 to the bayonet with an airtight seal.
- 672 ● The electrically driven stainless steel centrifugal pump installed to transfer
673 the water has a capacity of 120-300 l min⁻¹.
- 674 ● All accessories in contact with water are stainless steel with a sanitary finish
675 to prevent corrosion and formation of bacterial colonies.

676 The recirculation system of the water plant is used to fill the transport tank.
677 This allows a flow of 12 500 l in 50 minutes. Before filling the tank the water
678 conductivity is tested with a hand-held conductivity meter. To fill the detec-
679 tors, hatch covers are removed after cleaning the tank surface, one liner cap
680 is opened and the bayonet, after being rinsed thoroughly, is introduced into
681 the liner and screwed to the liner opening, and the pump is turned on. A
682 second liner port is opened for air release. The filling of the detector takes
683 approximately 45 minutes. The height of the water column is determined by
684 measuring the height of the tank and subtracting the height of the water
685 level, measured from the top of the tank. This gives a precision of 1-2 cm. The
686 level is measured at different hatch openings to avoid systematic errors due
687 to any possible tank tilt. After filling, any remaining air is pumped out of the
688 liners with a vacuum cleaner. Once deployed, water level measurements can
689 be obtained from the slope of the charge histogram from single muon tracks
690 [24,25].

691 After pauses in water deployment of five to six days, the transport tanks and
692 all accessories are cleaned and disinfected, and filters are checked and replaced
693 as required. Cleaning is done with detergent, bleach and a very thorough rinse.

694 8 Maintenance and Operation

695 As of September 2007, more than 1400 surface detector stations are opera-
696 tional. Typically more than 98.5% of the stations are operational at any time.
697 The technical staff distributes its time between deployment of new detectors
698 and maintenance and repair of down stations.

699 Only seven liners were observed to leak shortly after installation. In these
700 cases, which constitute the worst failure mode, the tank is emptied and brought
701 back to the Assembly Building for replacement of the interior components.

702 There have been very few instances of human interference with the surface
703 detectors. During 5 years of operation, only 12 solar panels have been damaged
704 and two have been removed (both from locations along side a paved road).

705 Solar power system parameters are recorded and analyzed using the central
706 data acquisition system. Failures are treated on an individual basis. Moni-
707 toring software for the solar power system has been developed to make this
708 monitoring routine for operating personnel and scientists either on shift at the
709 site or elsewhere by internet access. The lifetime of batteries is estimated to
710 be four years. The batteries will be monitored along with the rest of the solar
711 power system. The condition of the batteries can be determined from the data
712 (voltages, currents, and temperatures) that are being monitored and the weak
713 batteries can therefore be identified weeks or even months before complete
714 failure occurs. Batteries can then be scheduled for replacement by the routine
715 maintenance process.

716 9 Conclusions

717 In conclusion, with over 1400 commissioned detectors in the field, some of
718 which have already been operational for over five years, much insight on their
719 performance has been gained. All components of the above-described detector
720 hardware have fully met our design expectations. The design has proven suf-
721 ficiently robust to withstand the adverse field conditions and failure rates are
722 less than expected. Data taking is ongoing and the first scientific results have
723 already been published. The physics performance has met or exceeded all of
724 our requirements [10,14,17,18].

725 Acknowledgements

726 The successful installation and commissioning of the Auger Surface Array
727 would not have been possible without the strong commitment and effort from
728 the technical and administrative staff in Malargüe.

729 We are very grateful to the following agencies and organizations for financial
730 support: Gobierno de la Provincia de Mendoza, Comisión Nacional de Energía
731 Atómica, Municipalidad de Malargüe, Fundación Antorchas, Argentina; the
732 Australian Research Council; Fundação de Amparo a Pesquisa do Estado de
733 São Paulo, Conselho Nacional de Desenvolvimento Científico e Tecnológico,
734 Fundação de Amparo a Pesquisa do Estado de Rio de Janeiro and Finan-
735 ciadora de Estudos e Projetos do Ministerio da Ciencia e Tecnologia, Brasil;
736 Ministry of Education, Youth and Sports of the Czech Republic; Centre Na-
737 tional de la Recherche Scientifique, Conseil Régional Ile-de-France, Départe-
738 ment Physique Nucléaire et Corpusculaire (PNC-IN2P3/CNRS), Departement
739 Sciences de l'Univers (SDU-INSU/CNRS), France; Bundesministerium für Bil-
740 dung und Forschung, Deutsche Forschungsgemeinschaft, Helmholtz-Gemein-
741 schaft Deutscher Forschungszentren, Finanzministerium Baden-Württemberg,
742 Ministerium für Wissenschaft und Forschung Nordrhein Westfalen, Ministerium
743 für Wissenschaft, Forschung und Kunst Baden-Württemberg, Germany; Isti-
744 tuto Nazionale di Fisica Nucleare and Ministero dell'Istruzione, dell'Università
745 e della Ricerca, Italy; Consejo Nacional de Ciencia y Tecnología Mexico;
746 Ministerie van Onderwijs, Cultuur en Wetenschap, Nederlandse Organisatie
747 voor Wetenschappelijk Onderzoek, Stichting voor Fundamenteel Onderzoek
748 der Materie, Netherlands; Ministry of Science and Higher Education, Poland;
749 Fundação para a Ciência e a Tecnologia, Portugal; Slovenian Ministry for
750 Higher Education, Science, and Technology and Slovenian Research Agency;
751 Comunidad de Madrid, Consejería de Educación de la Comunidad de Castilla
752 La Mancha, FEDER funds, Ministerio de Educación y Ciencia, Xunta de
753 Galicia, Spain; Science and Technology Facilities Council (formerly PPARC),
754 UK; the US Department of Energy, the US National Science Foundation, The
755 Grainger Foundation, U.S.A.; UNESCO and the ALFA-EC in the framework
756 of the HELEN Project.

757 References

- 758 [1] J. Linsley, Phys. Rev. Lett. **10**, 146-148 (1963)
759 [2] K. Greisen, Rev. Lett. **16**, 748 (1966)
760 [3] G.T. Zatsepin and V.A. Kuz'min, JETP Letters **4**, 78 (1966)
761 [4] M. Nagano and A.A. Watson, Rev. Mod. Phys. **72**, 689 (2000)

- 762 [5] Pierre Auger Observatory Design Report (March 1997), www.auger.org/admin
- 763 [6] The Pierre Auger Collaboration, “First Estimate of the Primary Cosmic Ray
764 Energy Spectrum Above 3 EeV from the Pierre Auger Observatory”, Proceedings
765 of the 29th International Cosmic Ray Conference, Pune, India, **7**, 387 (2005)
- 766 [7] M. Roth for the Pierre Auger Collaboration, “Measurement of the UHECR
767 energy spectrum using data from the Surface Detector of the Pierre Auger
768 Observatory”, Proceedings of the 30th International Cosmic Ray Conference,
769 Merida, Mexico (2007), H.E. 1.4.A - 313. arXiv:0706.2096v1 [astro-ph]
- 770 [8] M.A. Lawrence, R.J.O. Reid and A.A. Watson, *J. Phys. G* **17**, 733 (1991)
- 771 [9] T. Suomijarvi et. al. for the Pierre Auger Collaboration, “The Electronics System
772 of the Surface Detectors of the Pierre Auger Observatory”, in preparation.
- 773 [10] T. Suomijarvi for the Pierre Auger Collaboration, “Performance of the
774 Pierre Auger Observatory Surface Detector”, Proceedings of the 30th
775 International Cosmic Ray Conference, Mérida, Mexico (2007), H.E. 1.4.A - 299.
776 arXiv:0706.4322v1 [astro-ph]
- 777 [11] P. Facal San Luis for the Pierre Auger Collaboration, “Measurement of the
778 UHECR spectrum above 10^{19} eV at the Pierre Auger Observatory using showers
779 with zenith angles greater than 60° ”, Proceedings of the 30th International Cosmic
780 Ray Conference, Mérida, Mexico (2007), H.E. 1.4.A - 319. arXiv:0709.1823v1
781 [astro-ph]
- 782 [12] D. Allard et. al. for the Pierre Auger Collaboration, “Aperture calculation of the
783 Pierre Auger Observatory surface detector”, Proceedings of the 29th International
784 Cosmic Ray Conference, Pune, India, **7**, 71 (2005)
- 785 [13] I. Allekotte et. al., *J. Phys. G: Nucl. Part. Phys.* **28**, 1499 (2002)
- 786 [14] P. Ghia for the Pierre Auger Collaboration, “Statistical and systematic
787 uncertainties in the event reconstruction and S(1000) determination by the Pierre
788 Auger surface detector”, Proceedings of the 29th International Cosmic Ray
789 Conference, Pune, India, **7**, 167 (2005)
- 790 [15] M. Ave et. al. for the Pierre Auger Collaboration, *Nucl. Inst. & Meth.* **A578**,
791 180 (2007)
- 792 [16] C. Bonifazi, A. Letessier-Selvon and E. M. Santos, accepted in *Astrop. Phys.*
793 (2007), astro-ph 0705.1856.
- 794 [17] C. Bonifazi for the Pierre Auger Collaboration, “Angular Resolution of the
795 Pierre Auger Observatory”, Proceedings of the 29th International Cosmic Ray
796 Conference, Pune, India, **7**, 17 (2005)
- 797 [18] M. Ave for the Pierre Auger Collaboration, “Reconstruction accuracy of the
798 surface detector array of the Pierre Auger Observatory”, Proceedings of the 30th
799 International Cosmic Ray Conference, Merida, Mexico (2007), H.E. 1.4.A - 297.

- 800 [19] M. Aglietta et. al. for the Pierre Auger Collaboration, “Response of the Pierre
801 Auger Observatory Water Cherenkov Detectors to Muons”, Proceedings of the
802 29th International Cosmic Ray Conference, Pune, India, **7**, 83 (2005)
- 803 [20] X. Bertou et. al. for the Pierre Auger Collaboration, Nuclear Instruments and
804 Methods in Physics Research **A568** 839 (2006)
- 805 [21] The Pierre Auger Collaboration, Nucl. Instr.& Meth. A **523** 50-95 (2004)
- 806 [22] A. Filevich et. al., Nucl. Inst. & Meth. **A423**, 69 (1999)
- 807 [23] J. Ogwoka Gichaba, “Measurements of Tyvek Reflective Properties for
808 the Pierre Auger Project,” University of Mississippi Masters Thesis (1998).
809 <http://lss.fnal.gov/archive/masters/fermilab-masters-1998-05.pdf>
- 810 [24] I. Allekotte et. al. for the Pierre Auger Collaboration, “Observation of the
811 Long Term Stability of Water Stations in the Pierre Auger Surface Detector”,
812 Proceedings of the 29th International Cosmic Ray Conference, Pune, India, **8**,
813 287 (2005)
- 814 [25] P. Allison et. al. for the Pierre Auger Collaboration, “Observing muon decays
815 in water Cherenkov detectors at the Pierre Auger Observatory”, Proceedings of
816 the 29th International Cosmic Ray Conference, Pune, India, **8**, 299 (2005)